Management of Harmonic Propagation in a Marine Vessel by use of Optimization

Espen Skjong
Center for Autonomous Marine Operations and Systems, Department of Engineering Cybernetics, Norwegian University of Science and Technology / Ulstein Power & Control AS
Email: espen.skjong@ulstein.com

Miguel Ochoa-Gimenez
Department of Engineering Cybernetics, Comillas Pontifical University
Email: miguel.ochoa@iit.upcomillas.es

Marta Molinas
Department of Engineering Cybernetics, Norwegian University of Science and Technology
Email: marta.molinas@ntnu.no

Tor Arne Johansen
Center for Autonomous Marine Operations and Systems, Department of Engineering Cybernetics, Norwegian University of Science and Technology
Email: tor.arne.johansen@ntnu.no

***Abstract*—Advances in power electronics drive systems for variable speed operation has enabled extensive use of such solutions in the propulsion and thruster systems of marine vessels. These solutions however introduce current and voltage distortions that compromises the overall power quality of the onboard electrical system. This paper presents and discusses one approach for generating the harmonic current reference for an active filter based on optimization. Two relevant results are revealed by this study: 1) lower THD values are attained by performing system optimization compared to local compensation of one load, and 2) the lower THD values are achieved with a smaller active filter rating than the one required for local load compensation.**

I. Introduction

Harmonics pollution in the voltage caused by the presence of non-linear loads in the onboard electrical system has become a major power quality issue in marine vessels. Up to 80% of the load in a marine vessel are non-linear due to the extensive use of variable speed drives in the electrical propulsion systems with a resulting Total Harmonic Distortion (THD) in the voltage that can exceed 20% [1].

Variable speed drive (VSD) systems operating the electrical propulsion in a vessel will extract non-sinusoidal currents from the electrical generators and these currents by flowing through the electrical system will create voltage distortions that can exceed acceptable levels by the classification entities. [2].

Figure 1 shows the single line diagram of the main power installations in a vessel with a typical diesel-electric propulsion. The main components being electric power generation, electric power distribution, VSD motor drive systems for main propulsion/thrusters and ship service distribution. Typical VSD systems are composed by a front end diode rectifier that will extract current with characteristic harmonics of the 5th, 7th, 11th and 13th, etc. (6 pulse rectifier), and of the 11th, 13th, 23th, 25th, etc. (12 pulse rectifier). 18-pulse drive systems also exists and up to 48 pulse systems are reported for very large systems. Increasing the pulse number can reduce the total harmonic distortion in the current by exploiting the cancellation effect of the phase shifting transformer. However, measurement of harmonics in the field reveal the presence of non-characteristic harmonics due to the effect of transformer saturation and voltage unbalances [3]. In general, the

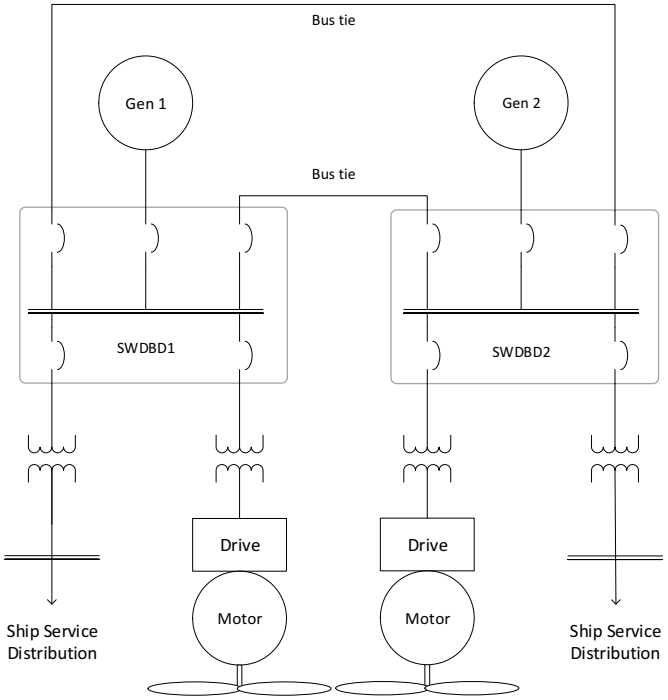

Fig. 1: Simplified single line diagram of the marine vessel electrical distribution under investigation.

spectrum of harmonic distortion in the voltage and currents will depend not only on the characteristic harmonics of the given configuration and topology of the VSD, but also on transformer saturation and loading of the 3 phase system. This will complicate the task of a-priori knowing (identifying) the specific composition of harmonics in the voltage and currents. Still, most harmonic compensation approaches will generally require the knowledge of the harmonic composition to be able to achieve a targeted (selective/proper) reduction of the THD.

The most widespread approach for mitigating harmonics is the use of passive filters. Passive filters are typically tuned to absorb a given set of harmonics and the configuration needs to be modified if the harmonic spectrum changes. Active filters, which are based on PWM harmonic current injection, have

a broadband compensation capability and can follow in real-time changes in the harmonic spectrum due to their inherent fast current tracking performance. This property makes them perfectly suited for tightly following dynamic loads. The downside is that active filter technology is costly and more complex than passive filters. The cost of the technology increases as the required power rating gets higher [4]. Therefore, achieving a given THD performance with a small filter size is a highly desirable objective that has been the main motivation of this investigation.

Due to cost, complexity and reliability issues, active filters are generally not considered as first candidate solution for harmonic compensation in marine vessels. A reason behind this might lie in the fact that active filters were traditionally designed for locally compensating residual harmonics of large industrial loads in combination with passive filters. Active filters are not generally proposed for global or system-wide mitigation of harmonics. In this paper, we explore and investigate the capabilities offered by the active filter with its embedded digital control and fast switching actions to perform the task of system-wide harmonics mitigation in a marine vessel. As the compensation problem becomes more complex when addressing harmonic compensation at the system level with a minimum required filter size that can meet the compensation target, it is natural to approach the problem using optimization techniques.

Ideally, an active filter can always produce the harmonic current waveform required by the load so that the source will only provide the fundamental current. However, this will require a filter current rating that can be prohibitively expensive. In addition, when there is more than one harmonic generating load, the concept of perfect compensation of one load will, in general, provide a non-optimal compensation to the overall system. These two aspects (system level THD reduction and minimum filter size) are simultaneously addressed in this paper by formulating an optimization problem that includes both, system THD and filter size, in the objective function.

The optimization problem is formulated in a way that the algorithm is searching for the best combination of current harmonic phases that will give as a solution the best feasible THDs in the system with the minimum required rating for the active filter. The findings of the optimization methodology that is elaborated in the subsequent sections are promising and reveal a lower system THD and filter rating than achievable with local compensation without optimization.

II. Marine vessel system modelling

A marine vessel's power distribution grid is designed to handle loss of power caused by e.g. short circuited distribution lines, various faults related to loads, and tripping of generators. This is often achieved by advanced power grid designs using bus-tie breakers [5]. The simplified model of a small distribution grid shown in figure 2 (parameters represented in table I) is assumed in this paper. This model includes two generators, two loads and an active harmonic filter.

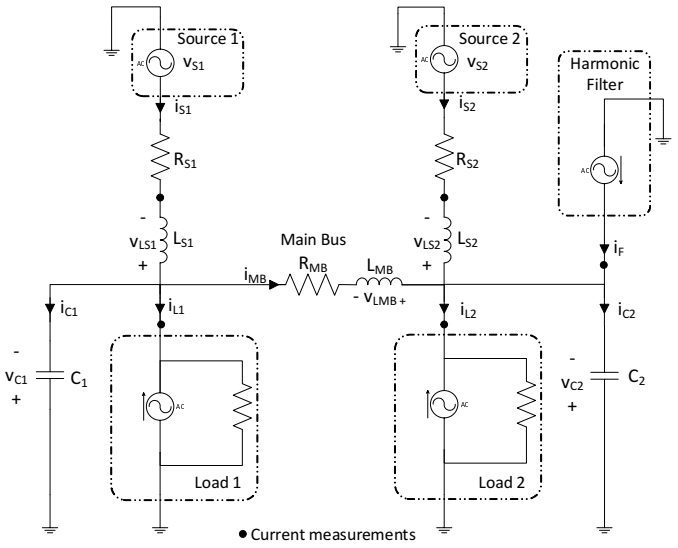

Fig. 2: Equivalent electrical circuit configuration of the power distribution grid model under investigation.

Parameter	Value
L_{S1}	1 mH
L_{S2}	1 mH
L_{MB}	1 mH
R_{S1}	$(0.1 \cdot L_{S1} \cdot \omega)\ \Omega$
R_{S2}	$(0.1 \cdot L_{S2} \cdot \omega)\ \Omega$
R_{MB}	$(0.1 \cdot L_{MB} \cdot \omega)\ \Omega$
C_1	0.1 μF
C_2	0.1 μF

TABLE I: Electrical distribution system parameters.

A. Model of the Power Distribution Grid

The mathematical model for the power distribution grid illustrated in figure 2 can be derived using Kirchhoff's current and voltage laws, and can be stated as

$$\begin{aligned} L_{S1}\frac{di_{S1}}{dt} &= v_{S1} - R_{S1}i_{S1} - v_{C1} \\ C_1\frac{dv_{C1}}{dt} &= i_{S1} - i_{MB} - i_{L1} \\ L_{MB}\frac{di_{MB}}{dt} &= v_{C1} - v_{C2} - R_{MB}i_{MB} \\ C_2\frac{dv_{C2}}{dt} &= i_{MB} + i_{S2} - i_{L2} + i_F \\ L_{S2}\frac{di_{S2}}{dt} &= v_{S2} - R_{S2}i_{S2} - v_{C2}, \end{aligned} \tag{1}$$

One should note that capacitors are inserted in the power grid for modeling purposes, and should be given small values with the only purpose of having a well-defined solution to the equations, e.g. 10^{-7} F.

The generators are modeled as ideal voltage sources with a voltage phase shift ϕ_V,

$$v_S(t) = \sqrt{2}V_{rms}\sin(\omega t + \phi_V), \tag{2}$$

while the nonlinear loads are modeled as current sources with characteristic harmonic components of order 5, 7, 11 and 13

with phase shifts $\phi_{L,i}$ and amplitudes $I_{L,i}$,

$$i_L(t) = \sum_i I_{L,i} \sin\left(i(\omega t + \phi_{L,i})\right), \quad \forall i \in \{1, 6k \pm 1 | k = 1, 2\}. \tag{3}$$

The fundamental frequency can also experience variations due to unbalances between produced and consumed power, which introduces speed variations in the generator shafts. Such variations can be represented by including in the model of the currents the following expression

$$f(t) = f_f + A_p \sin\left(2\pi f_t t\right), \tag{4}$$

where f_f is the fundamental frequency, A_p is the frequency variation peak and f_t is the rate of the frequency variations. The rate of the frequency variations, f_t, is often within 0.1-1 Hz, and the frequency peak, A_p, is assumed to be 1-5 Hz. Hence, the time varying angular frequency is given by $\omega := \omega(t) = 2\pi f(t)$.

B. Model of the Active Filter (AF)

The active filter is modeled as a current source as indicated in figure 2. The operation of the AF is based on the principle of locally supplying to the load the higher order harmonic components of the load current so that the generators will only supply a clean sinusoidal current to the load. In this way, the active filter harmonic current injection will mitigate the propagation of harmonics through the vessels distribution grid. The mathematical expression of the AF harmonic current injection is

$$i_F(t) = \sum_i I_{F,i} \sin\left(i(\omega t + \phi_{F,i})\right), \quad \forall i \in \{6k \pm 1 | k = 1, 2\}, \tag{5}$$

where $I_{F,i}$ are amplitudes of the filter's harmonic current components. Before proceeding with the discussion of harmonic filter constraints, the power grid model should be extended to a three-phase three-wire configuration.

Due to the properties of three-phase three-wire the $\alpha\beta 0$ frame is simplified to $\alpha\beta$, where the β current is lagging the α current by 90°. This is due to the assumption of balanced sources, hence the neutral wire in a three-phase four-wire configuration is excessive. The three-phase three-wire model for the voltage sources, assuming balanced sources, can be written in the $\alpha\beta$ frame as

$$\mathbf{v}_S(t) = \begin{bmatrix} v_{S,\alpha}(t) \\ v_{S,\beta}(t) \end{bmatrix} = \begin{bmatrix} \sqrt{3} V_{rms} \sin(\omega t + \phi_V) \\ \sqrt{3} V_{rms} \sin(\omega t + \phi_V + \frac{\pi}{2}) \end{bmatrix}. \tag{6}$$

In the same way, the load and filter models can be extended to three-phase three-wire using the $\alpha\beta$ frame. Due to the definition of the $\alpha\beta$ frame, which requires 90° phase between the α and the β phase, all load and filter phases ($\phi_{F,i}$ and $\phi_{L,i}$) must be equal for both α and β phase. Aslo, for the filter model (eq. (5)), the filter amplitudes in α and β are kept equal to ensure balanced filter currents.

In the rest of this paper subscript α and β are used to denote the α and β phases for each voltage and current component, and the vectors (phasors) $\mathbf{v}$ and $\mathbf{i}$ are used to represent voltages and currents, respectively, given in the $\alpha\beta$ frame. It is referred to [6] for details regarding the $\alpha\beta$ frame in three-phase three-wire configurations.

C. Model of the AF Current Rating Constraints

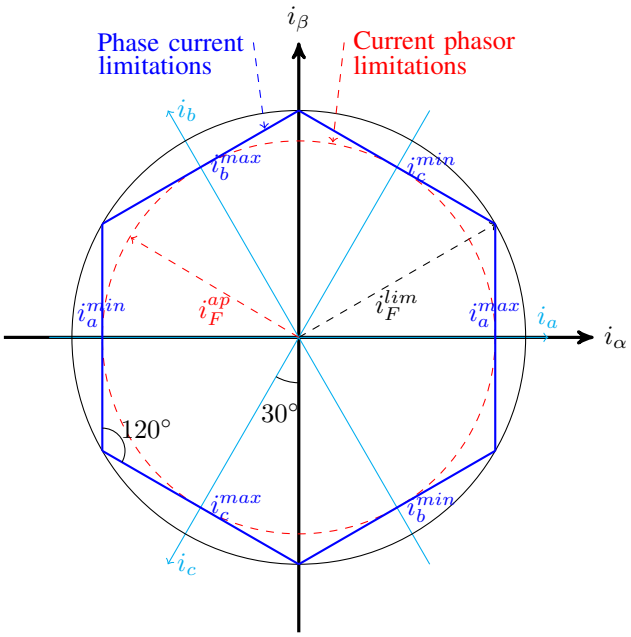

Fig. 3: Harmonic filter constraints: Three-phase three-wire represented by the $\alpha\beta$ transform [7].

The harmonic filter model should be constrained to the filter's physical limitations. Figure 3 illustrates the limitations in both the abc and the $\alpha\beta$ frames. In the abc frame the phases are restricted by

$$i_j^{min} \leq i_j \leq i_j^{max}, \quad \forall j \in \{a, b, c\}, \tag{7}$$

which forms the hexagon given in figure 3. These restrictions can be expressed in the $\alpha\beta$ form by

$$-i_F^{lim} \leq -i_{F,\beta} + \frac{\sqrt{3}}{3} i_{F,\alpha} \leq i_F^{lim} \tag{8a}$$

$$-i_F^{lim} \leq i_{F,\beta} + \frac{\sqrt{3}}{3} i_{F,\alpha} \leq i_F^{lim} \tag{8b}$$

$$-i_F^{ap} \leq i_{F,\alpha} \leq i_F^{ap} \tag{8c}$$

$$-i_F^{lim} \leq i_{F,\beta} \leq i_F^{lim}, \tag{8d}$$

where the hexagon's apothem is given by

$$i_F^{ap} = \sqrt{\left(i_F^{lim}\right)^2 - \left(\frac{i_F^{lim}}{2}\right)^2} = \frac{\sqrt{3}}{2} i_F^{lim}, \tag{9}$$

and i_F^{lim} is a design variable representing the filter's limitations. Eq. (8) gives a set of linear constraints, which represent the physical limitations of the filter. An approximation of the hexagon constraints, which is given by the red dotted circle in figure 3, is given by

$$0 \leq \left(i_{F,\alpha}\right)^2 + \left(i_{F,\beta}\right)^2 \leq \left(i_F^{ap}\right)^2. \tag{10}$$

The current phasor constraint given by eq. (10) is nonlinear and may increase the required calculation costs to find an optimal solution to the problem. The circular constraints, eq. (10), will be used in the test cases presented in section IV due to simplicity of implementation. For notational simplicity we define the feasible region for the filter's current vector $\mathbf{i}_F \in \mathbb{S}$.

III. Formulation of the Optimization Problem

The overall goal of the optimization is to minimize the harmonic distortions in the power grid by controlling the harmonic filter's amplitudes and phases. One approach to optimize filter currents is the Nonlinear Model Predictive Control (NMPC). The NMPC approach re-optimizes the filter currents after each completed optimization horizon using new measurements as initial values to the optimization problem. In this paper the NMPC problem is solved using *Multiple Shooting* and a non-linear programming (NLP) solver. Before discussing multiple shooting, the problem is formulated on standardized form.

A. Algorithm of the Objective Function

In order to perform this study, the indicator used for the system level THD, is defined as a function of the sum of all the harmonic currents in the system. Aiming at minimizing this function, will in turn reduce the THD of all currents in the system and by that the THD of the load voltages.

The objective of the problem will therefore be to minimize, by design, the harmonic current components generated by each non-linear load, and by that prevent harmonic distortions from propagating through the power distribution grid. Assuming that the higher order harmonics (5th, 7th, 11th and 13th) generated by a 6-pulse diode rectifier are known and given by

$$\begin{aligned}\mathbf{i}_L^{hh} = &\begin{bmatrix} \sum_i I_{L,\alpha,i} \sin\left(i(\omega t + \phi_{L,\alpha,i})\right) \\ \sum_i I_{L,\beta,i} \sin\left(i(\omega t + \phi_{L,\beta,i} + \frac{\pi}{2})\right) \end{bmatrix}, \\ &\forall i \in \{6k \pm 1 | k = 1, 2\},\end{aligned} \tag{11}$$

and the algebraic state vector can be represented by

$$\mathbf{z} = \left[\mathbf{v}_{S1}^\top, \mathbf{v}_{S2}^\top, \mathbf{i}_{L1}^\top, \mathbf{i}_{L2}^\top, \mathbf{i}_F^\top, (\mathbf{i}_{L1}^{hh})^\top, (\mathbf{i}_{L2}^{hh})^\top\right]^\top, \tag{12}$$

where the loads $\mathbf{i}_{L1}$ and $\mathbf{i}_{L2}$ are the three-phase three-wire extension of eq. (3) given in the $\alpha\beta$ frame, the filter current $\mathbf{i}_F$ is the three-phase three-wire extension of eq. (5) given in the $\alpha\beta$ frame, and the harmonic components of each load, $\mathbf{i}_{L1}^{hh}$ and $\mathbf{i}_{L2}^{hh}$, are given by eq. (11). The dynamic state vector is given by

$$\mathbf{x} = \left[\mathbf{i}_{S1}^\top, \mathbf{i}_{S2}^\top, \mathbf{i}_{MB}^\top, \mathbf{v}_{C1}^\top, \mathbf{v}_{C2}^\top\right]^\top. \tag{13}$$

To control the filter currents, both filter amplitudes and phases are considered as controls, which can be altered during the optimization horizon, thus time dependent. Hence, the control vector is stated as

$$\mathbf{u} = \left[I_{F,i}, \phi_{F,i}\right]^\top, \quad \forall i \in \{6k \pm 1 | k = 1, 2\}. \tag{14}$$

The NMPC problem can now be stated on a horizon T as

$$\begin{aligned}\min_{\mathbf{u}} \quad & V(\mathbf{x}, \mathbf{z}, \mathbf{u}, t) = \int_0^T l(\mathbf{x}(t), \mathbf{z}(t), \mathbf{u}(t)) dt \\ \text{s.t.} \quad & \\ & \dot{\mathbf{x}}(t) = \mathbf{f}(\mathbf{x}(t), \mathbf{z}(t), \mathbf{u}(t)), \\ & \mathbf{h}(\mathbf{x}(t), \mathbf{z}(t), \mathbf{u}(t)) = 0, \\ & \mathbf{g}(\mathbf{x}(t), \mathbf{z}(t), \mathbf{u}(t)) \leq 0, \quad \forall t \in [0, T] \\ & \text{given initial values } \mathbf{x}(0), \mathbf{z}(0) | \mathbf{i}_F(0) \in \mathbb{S}.\end{aligned} \tag{15}$$

$\mathbf{h}(\cdot)$ and $\mathbf{g}(\cdot)$ represents equality and inequality constraints, respectively. By dropping the time notation (t), the stage cost function $l(\cdot)$ minimizing the harmonic distortions close to the loads, with constant weights q_1, q_2, q_u, is

$$\begin{aligned}l(\mathbf{x}, \mathbf{z}, \mathbf{u}) = & q_1 \left(i_{F,\alpha} - i_{L1,\alpha}^{hh}\right)^2 + q_1 \left(i_{F,\beta} - i_{L1,\beta}^{hh}\right)^2 \\ & + q_2 \left(i_{F,\alpha} - i_{L2,\alpha}^{hh}\right)^2 + q_2 \left(i_{F,\beta} - i_{L2,\beta}^{hh}\right)^2 \\ & + q_u \left(\mathbf{u}_{I_F}^\top \mathbf{u}_{I_F}\right).\end{aligned} \tag{16}$$

$\mathbf{u}_{I_F} = \mathbf{Q}\mathbf{u}$ contains the filter's amplitudes. The last part in eq. (16) is added to minimize the filter amplitudes, hence minimizing the filter's power rating, and also provide stability and robustness with regards to modeling errors. $q_u < q_1, q_2$ as minimizing the power rating is of lesser importance than decreasing the harmonic pollution in the power grid.

B. Direct Multiple Shooting

Non-linear Programming solvers requires a problem formulation consisting of a set of equations dependent only on the unknown control variables. Multiple shooting is one of many methods which integrate, discretize and reshapes the problem formulation to a form accepted by NLP solvers [8, 9, 10]. In the multiple shooting method the time domain is divided into smaller time intervals and the DAE (Differential Algebraic Equation) models are integrated separately in each interval. In direct multiple shooting the controls are discretized on the coarse grid given by each interval. To provide continuity of the states across intervals, equality constraints are imposed. If we denote the dynamic state vector $\mathbf{x}$ at the start of interval n as $\mathbf{x}_n(t_{n,0})$ and end of the interval as $\mathbf{x}_n(t_{n,1})$, the equality constraints which binds the intervals $n \in N$ are

$$\mathbf{x}_{n-1}(t_{n-1,1}) - \mathbf{x}_n(t_{n,0}) = 0, \quad n = 2, \ldots, N, \tag{17}$$

where $\mathbf{x}_1(0) = \mathbf{x}_0$, $\mathbf{x}_0$ initial value. The equality constraints, eq. (17), are added to the NLP formulation defined in eq. (15). The integration scheme used in the multiple shooting in this work is the explicit *Runge-Kutta 4* (RK4) [8, ch. 9].

C. Implementation Aspects and Requirements

The implementation of the NMPC is realized in Python using the `Casadi` framework, which is a symbolic framework for algorithmic differentiation and numeric optimization [11]. The NLP solver used is IPOPT [12]. Due to the modeled frequency variations in the fundamental frequency the MPC is scheduled to provide a filter current reference lasting 0.025s, which is a little bit longer than one period of 50Hz. The NMPC

implementation for the test cases represented in this paper uses a couple of seconds (Intel Core i7-4600U CPU @ 2.10GHz $\times$ 4) to solve one period of the horizon, i.e. 0.02 seconds horizon at 50 Hz. Clearly, the Python implementation does not provide sufficient real-time properties suitable for solving the optimization problem, and thereby only used for prototyping in a simulation environment.

Despite the large optimization problem and the computational costs related to the Python implementation putting the real-time properties at risk for a practical implementation of the NMPC, the solution could be implemented in C/C++ which may give better real-time properties. Another possibility is to use a FPGA to solve the optimization problem. The FPGAs are quite effective and have shown promising results related to linear and nonlinear MPC implementations, [13, 14]. FPGAs solving MPC problems have also been used for controlling power electronics, which requires low computational costs [15].

IV. Results

Three symmetric test cases with different levels of harmonic distortions are studied. Table II summarizes the test cases corresponding to a 6-pulse diode rectifier for load 1 and load 2.

TABLE II: Test cases for 6-pulse diode rectifier loads.

	Load Amplitudes [pu] [1th, 5th, 7th, 11th, 13th]	**Load Phases** [pu] [1th, 5th, 7th,... 11th, 13th]	**Frequency Model**
Case 1	$\imath^{\alpha}_{L1} = \imath^{\beta}_{L1} = \imath^{\alpha}_{L2} = \imath^{\beta}_{L2} = [0.9, 0.3, 0.1, 0, 0]$	$\phi_L = [0, 0, 0, 0, 0]$	$f_f = 50$ Hz $A_p = 2$ Hz $f_t = 0.5$ Hz
Case 2	$\imath^{\alpha}_{L1} = \imath^{\beta}_{L1} = \imath^{\alpha}_{L2} = \imath^{\beta}_{L2} = [0.9, 0.4, 0.1, 0, 0]$	$\phi_L = [0, 0, 0, 0, 0]$	$f_f = 50$ Hz $A_p = 2$ Hz $f_t = 0.5$ Hz
Case 3	$\imath^{\alpha}_{L1} = \imath^{\beta}_{L1} = \imath^{\alpha}_{L2} = \imath^{\beta}_{L2} = [0.9, 0.5, 0.1, 0, 0]$	$\phi_L = [0, 0, 0, 0, 0]$	$f_f = 50$ Hz $A_p = 2$ Hz $f_t = 0.5$ Hz

Before addressing the resulting THD values for the voltages near the loads the necessary current filter rating to perform sufficient harmonic conditioning is discussed.

A. Active Filter Required Current Rating

Figure 4 showcases different filter current ratings for each test case proposed in table II. As evident the THD values are smallest when the filter's current limit, i_F^{lim}, becomes large enough to cope with the harmonic pollution from the nonlinear loads. Due to the difference in harmonic pollution the test cases requires different filter current limits to cope with the harmonics. For test case 1 a current limit of $i_F^{lim} = 0.5$ [pu] is sufficient. An increase in the current limit would not give better THD values. The same applies for test case 2 and 3 which have current limits of approximately $i_F^{lim} = 0.6$ [pu] and $i_F^{lim} = 0.7$ [pu], respectively. Even at low current ratings the filter would conduct harmonic conditioning. As can be seen from test case 3 in figure 4 a current rating of $i_F^{lim} = 0.1$ [pu] is too low to cope with the high level of harmonic pollution, however the filter reduces the THD values for the voltages near the loads even at this low current rating. The findings tied to the THD saturation, as showcased in figure 4, would be important when deciding the filter size for power grids with certain levels of harmonic pollution.

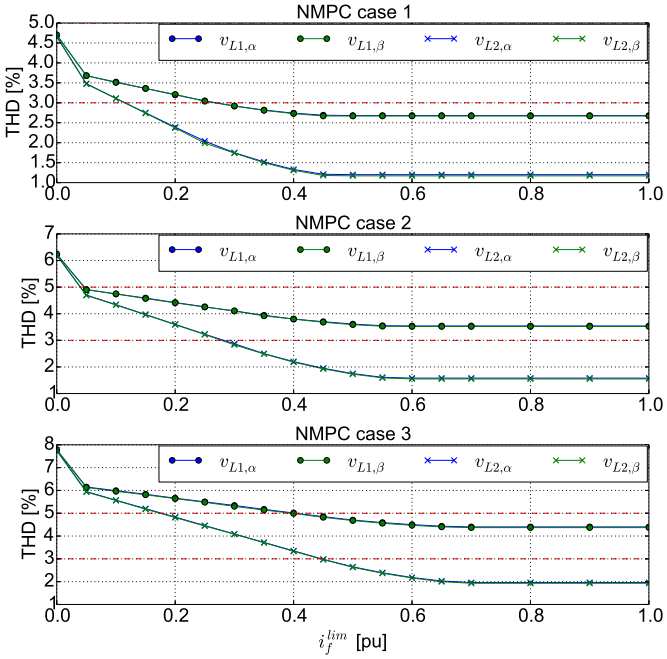

Fig. 4: Active filter required current rating versus Total Harmonic Distortions.

B. Total Harmonic Distortion in the system

Another result to be discussed is the resulting THD values for the voltages near the nonlinear loads, which are shown for all three cases in figure 5 with and without filtering. A local filter with infinite filter size has been added for comparison. The local filter considers only load 2 and has no further knowledge of the grid. The total THD values are computed using the THD from each phase in the $\alpha\beta$ form by $THD_{total} = \sqrt{THD_{\alpha}^2 + THD_{\beta}^2}$.

For all three test cases the THD values for the voltage near load 1, v_{L1}, are more or less similar compared to the THD values when using the local filter without optimization. This is due to the impedance in the distribution grid preventing the filter to do better harmonic conditioning. Also the THD value for the voltage near load 2, v_{L2}, for case 1 is quite similar to the THD value when using the local filter. However the THD value for v_{L2} are lower for case 2 and 3 when using NMPC compared to local filtering. This is because of the MPC's consideration of both loads, with the result of reducing the THD.

Figure 6 illustrates the effect of harmonic conditioning using NMPC for case 3. The four plots to the left represent the

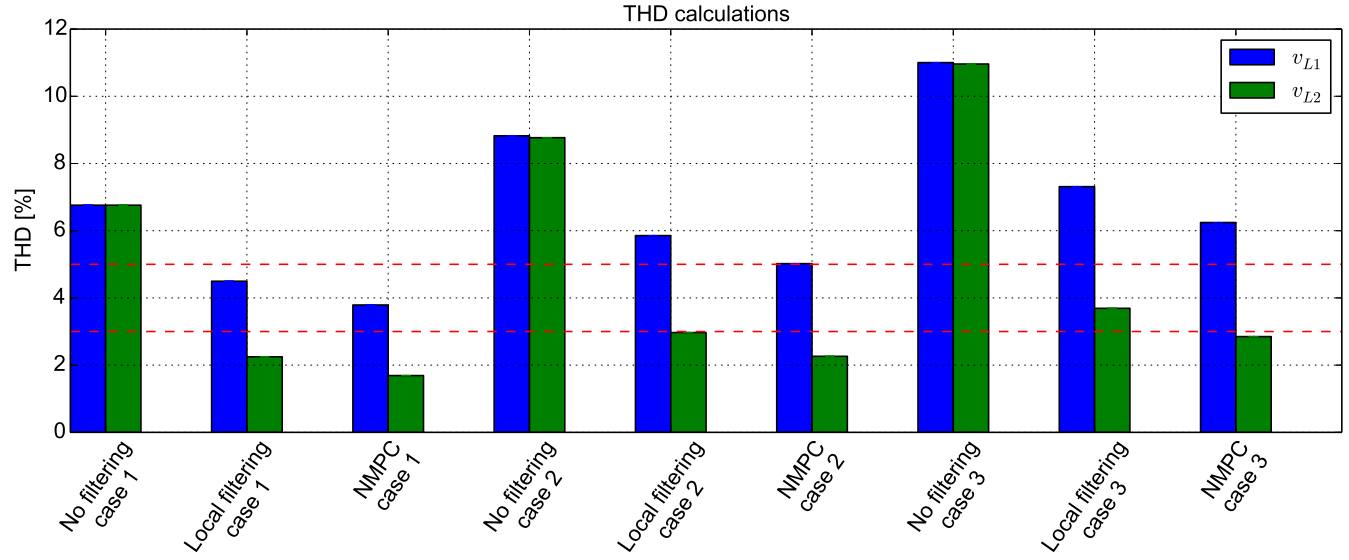

Fig. 5: Resulting THD from instantaneous filtering and optimization based active filter.

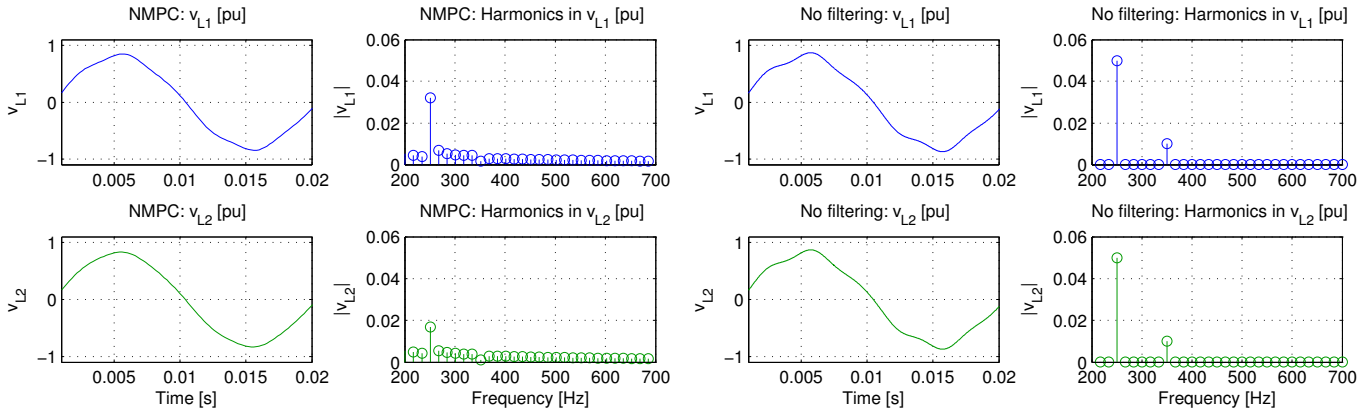

Fig. 6: Load voltages for case 3 with filtering (NMPC) and without filtering.

voltages v_{L1} and v_{L2} when using NMPC to provide filter reference currents, while the four plots to the right represent the voltages when no filtering is conducted. As can be seen, the harmonic components have been reduced, resulting in the decreased THD values represented in figure 5.

C. Active filter power rating

Since the NMPC optimizes the phases when calculating the optimal filter currents, also the filter's power rating will be lower compared to local filtering. This is illustrated in figure 7. As evident, when using the NMPC to calculate the active filter reference current a higher level of harmonic pollution will give a better power rating compared to local filtering. This is because filter amplitudes will generally be higher for a high level of harmonic pollution compared to a low level of harmonic pollution. Hence, utilizing the filter phases in the NMPC would result in using lower filter amplitudes than utilized by local filtering, which in turn would result in a lower filter power rating, as illustrated in figure 7.

V. Conclusion

This paper shows how optimization can be used to provide the reference current to an active filter for system level harmonic conditioning in a marine vessel's power grid. A non-linear model predictive control (NMPC) was proposed and implemented based on a simplified power distribution grid model, including the active filter's current constraints. Multiple shooting and the NLP solver IPOPT [12] was used to solve the NMPC problem.

Three test cases with different levels of symmetric loads were investigated, and local filtering was implemented for the purpose of comparison. It was shown that even with small filter ratings the active filter was able to achieve harmonic conditioning due to the flexibility of altering the filter current phases, and by that reducing the filter current amplitudes. The utilization of filter current phases resulted in a lower active filter rating when using the NMPC compared to local filtering.

Overall, the NMPC provides better harmonic conditioning than local filtering. This is because the NMPC considers

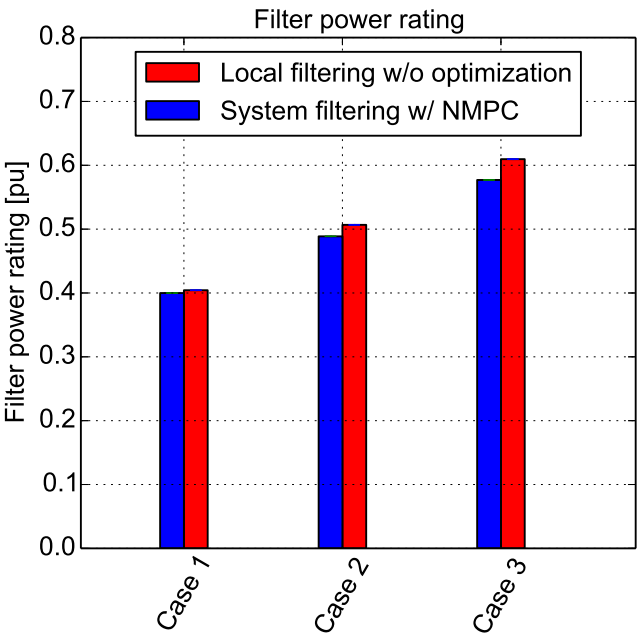

Fig. 7: Required filter power rating.

both sources and calculates optimal filter current references. However, only test cases with symmetrical loads were presented in this study. When asymmetrical loads are present, and especially if load 1 is more distorted than load 2, the NMPC is expected to provide even better harmonic conditioning than local filtering due to the consideration of both loads [16, 17].

A reduction in active filter power rating is sought for due to economical reasons. Hence, compared with local filtering, an active filter with NMPC calculated filter reference currents could provide better filtering with a lower power rating than using local filtering techniques.

The optimization-based filter current reference generation implementation presented in this work does not yet provide real-time properties enabling flexible, stable and robust power conditioning. One possible approach towards satisfactory real-time properties would be to model the filter currents, the load currents and source voltages as linear second order oscillations, and use the hexagon constraints which will result in a linear MPC representation. A linear MPC problem is generally easier to solve than a NMPC problem, and effective linear solvers like CVXGEN [18] and qpOASES [19] could provide the real-time properties needed. In the literature several linear MPC and linear optimization problem implementations, such as [15, 20, 21, 22, 23], are reported with good real-time properties. Another approach would be to use an effective C/C++ library, e.g. ACADO [24], to solve the NMPC problem discussed in this work.

Another important aspect to discuss is measurements and measurement noise. Measurements are required to initialize some of the variables in the algebraic state vector $\mathbf{z}$ and the dynamic state vector $\mathbf{x}$. Especially, the generator voltages, $\mathbf{v}_{S1}$ and $\mathbf{v}_{S2}$, and the load currents, $\mathbf{i}_{L1}$ and $\mathbf{i}_{L2}$, are necessary to initialize by measurements. These variables are fundamental entities and determines the grid's behavior at a given point of operation. The results of the harmonic conditioning using the MPC is depending on the accuracy and correctness of the load current measurements and the generator voltage measurements. Due to the MPC's predictive behavior measurements of the load amplitudes of each harmonic component, including the fundamental, are a necessity. These measurements can be obtained by real-time FFT measurement equipment, however, care must be taken since only a small deviation from the true measurement due to measurement noise could impair the quality of the harmonic conditioning. This could lead to THD values higher than the allowed limits set by class entities and also in worst case cause instability.

Acknowledgement

This work has been carried out at the Centre for Autonomous Marine Operations and Systems (AMOS). The Norwegian Research Council is acknowledged as the main sponsor of AMOS. This work was supported by Ulstein Power & Control AS and the Research Council of Norway, Project number 241205.

References

[1] I. Evans, A. Hoevenaars, and P. Eng, "Meeting harmonic limits on marine vessels," in *Electric Ship Technologies Symposium, 2007. ESTS '07. IEEE*, May 2007, pp. 115–121.

[2] DNV-OS-D201, "Electrical installations, offshore standards," Jan. 2005.

[3] S. Bourguet, P. Guerin, and R. LeDoeuff, "Non-characteristic harmonics generated by frequency converter," GE44 , Laboratory, Saint-Nazaire, France, All Electric Ship 2003, Edinbugh., 2003.

[4] H. Akagi, "Active harmonic filters," *Proceedings of the IEEE*, vol. 93, no. 12, pp. 2128–2141, Dec 2005.

[5] M. Patel, *Shipboard Electrical Power Systems*, ser. Shipboard Electrical Power Systems. Taylor & Francis, 2011.

[6] H. Akagi, E. Watanabe, and M. Aredes, *Instantaneous Power Theory and Applications to Power Conditioning*, ser. IEEE Press Series on Power Engineering. Wiley, 2007.

[7] J. A. Suul, "Control of Grid Integrated Voltage Source Converters under Unbalanced Conditions," PhD thesis, Norwegian University of Science and Technology, Department of Electrical Power Engineering, March 2012.

[8] L. Biegler, *Nonlinear Programming: Concepts, Algorithms, and Applications to Chemical Processes*, ser. MOS-SIAM Series on Optimization. Society for Industrial and Applied Mathematics (SIAM, 3600 Market Street, Floor 6, Philadelphia, PA 19104), 2010.

[9] M. Diehl, H. Bock, H. Diedam, and P.-B. Wieber, "Fast direct multiple shooting algorithms for optimal robot control," in *Fast Motions in Biomechanics and Robotics*, ser. Lecture Notes in Control and Information Sciences,

M. Diehl and K. Mombaur, Eds. Springer Berlin Heidelberg, 2006, vol. 340, pp. 65–93.

[10] H. Bock, M. Diehl, D. Leineweber, and J. Schlder, "A direct multiple shooting method for real-time optimization of nonlinear dae processes," in *Nonlinear Model Predictive Control*, ser. Progress in Systems and Control Theory, F. Allgöwer and A. Zheng, Eds. Birkhäuser Basel, 2000, vol. 26, pp. 245–267.

[11] J. Andersson, "A General-Purpose Software Framework for Dynamic Optimization," PhD thesis, Arenberg Doctoral School, KU Leuven, Department of Electrical Engineering (ESAT/SCD) and Optimization in Engineering Center, Kasteelpark Arenberg 10, 3001-Heverlee, Belgium, October 2013.

[12] A. Wächter and L. T. Biegler, "On the implementation of an interior-point filter line-search algorithm for large-scale nonlinear programming," *Mathematical Programming*, vol. 106, no. 1, pp. 25–57, 2006.

[13] K. Ling, S. Yue, and J. Maciejowski, "A fpga implementation of model predictive control," in *American Control Conference, 2006*, June 2006, pp. 6 pp.–.

[14] F. Xu, H. Chen, W. Jin, and Y. Xu, "Fpga implementation of nonlinear model predictive control," in *The 26th Chinese Control and Decision Conference (2014 CCDC),*, May 2014, pp. 108–113.

[15] P. Lezana, R. Aguilera, and D. Quevedo, "Model predictive control of an asymmetric flying capacitor converter," *IEEE Transactions on Industrial Electronics,*, vol. 56, no. 6, pp. 1839–1846, June 2009.

[16] E. Skjong, M. Molinas, and T. A. Johansen, "Optimized current reference generation for system-level harmonic mitigation in a diesel-electric ship using non-linear model predictive control," in *IEEE 2015 International Conference on Industrial Technology, ICIT*, March 2015.

[17] E. Skjong, M. Molinas, T. A. Johansen, and R. Volden, "Shaping the current waveform of an active filter for optimized system level harmonic conditioning," in *International Conference on Vehicle Technology and Intelligent Transport Systems, VEHITS*, May 2015.

[18] J. Mattingley and S. Boyd, "Cvxgen: a code generator for embedded convex optimization," *Optimization and Engineering*, vol. 13, no. 1, pp. 1–27, 2012.

[19] H. Ferreau, C. Kirches, A. Potschka, H. Bock, and M. Diehl, "qpOASES: A parametric active-set algorithm for quadratic programming," *Mathematical Programming Computation*, vol. 6, no. 4, pp. 327–363, 2014.

[20] A. Domahidi, A. Zgraggen, M. Zeilinger, M. Morari, and C. Jones, "Efficient interior point methods for multistage problems arising in receding horizon control," in *IEEE Conference on Decision and Control (CDC)*, Maui, HI, USA, Dec. 2012, pp. 668 – 674.

[21] G. Frison, D. K. M. Kufoalor, L. Imsland, and J. Jørgensen, "Efficient implementation of solvers for linear model predictive control on embedded devices," in *Proceedings of 2014 IEEE International Conference on Control Applications (CCA)*, 2014, pp. 1954–1959.

[22] D. M. Kufoalor, S. Richter, L. Imsland, T. Johansen, M. Morari, and G. Eikrem, "Embedded Model Predictive Control on a PLC Using a Primal-Dual First-Order Method for a Subsea Separation Process," in *Mediterranean Conference on Control and Automation*, Palermo, Jun. 2014.

[23] T. Geyer, G. Papafotiou, and M. Morari, "Model predictive control in power electronics: A hybrid systems approach," in *44th IEEE Conference on Decision and Control 2005, and 2005 European Control Conference. CDC-ECC '05.*, Dec 2005, pp. 5606–5611.

[24] B. Houska, H. Ferreau, and M. Diehl, "An Auto-Generated Real-Time Iteration Algorithm for Nonlinear MPC in the Microsecond Range," *Automatica*, vol. 47, no. 10, pp. 2279–2285, 2011.